

# The GlueX Experiment in Hall-D

The GlueX Collaboration\*

The goal of the GlueX experiment is to provide critical data needed to address one of the outstanding and fundamental challenges in physics – the quantitative understanding of the confinement of quarks and gluons in quantum chromodynamics (QCD). Confinement is a unique property of QCD and understanding confinement requires an understanding of the soft gluonic field responsible for binding quarks in hadrons. Hybrid mesons, and in particular exotic hybrid mesons, provide the ideal laboratory for testing QCD in the confinement regime since these mesons explicitly manifest the gluonic degrees of freedom. Photoproduction is expected to be particularly effective in producing exotic hybrids but there is little data on the photoproduction of light mesons. GlueX will use the coherent bremsstrahlung technique to produce a linearly polarized photon beam. A solenoid-based hermetic detector will be used to collect data on meson production and decays with statistics after the first full year of running that will exceed the current photoproduction data in hand by several orders of magnitude. These data will also be used to study the spectrum of conventional mesons, including the poorly understood excited vector mesons. In order to reach the ideal photon energy of 9 GeV for this mapping of the exotic spectrum, 12 GeV electrons are required. This document updates the physics goals, the beam and apparatus of the GlueX detector in Hall-D since the original proposal to PAC 30 in 2006 was presented [1].

## I. INTRODUCTION

We believe that quantum chromodynamics (QCD) is the correct theory of the strong interactions, but while the interactions of quarks and gluons are well described at high energy, the situation at low energy remains challenging. The most obvious physical manifestation of QCD is the spectrum of particles that make up the universe we live in, (baryons and mesons), but QCD predictions for these are currently only possible using lattice techniques to numerically calculate them.

The observation, nearly four decades ago, that mesons are grouped in nonets, each characterized by unique values of  $J^{PC}$  spin ( $J$ ), parity ( $P$ ) and charge conjugation ( $C$ ) quantum numbers led to the development of the quark model. Within this picture, mesons are bound states of a quark ( $q$ ) and antiquark ( $\bar{q}$ ). The three light-quark flavors (up, down and strange) suffice to explain the spectroscopy of most but not all of the lighter-mass mesons (below 3 GeV/ $c^2$ ) that do not explicitly carry heavy flavors (charm or beauty).

Our understanding of how quarks form mesons has evolved within quantum chromodynamics (QCD) and we now expect a richer spectrum of mesons that takes into account not only the quark degrees of freedom but also the gluonic degrees of freedom. Gluonic mesons with no quarks (glueballs) are expected. These are bound states of pure glue and since the quantum numbers of low-lying glueballs (below 4 GeV/ $c^2$ ) are not exotic, they should manifest themselves as extraneous states that cannot be accommodated within  $q\bar{q}$  nonets. But their unambiguous

identification is complicated by the fact that they can mix with  $q\bar{q}$ . Excitations of the gluonic field binding the quarks can also give rise to so-called hybrid mesons that can be viewed as bound states of a quark, antiquark and valence gluon ( $q\bar{q}g$ ).

An alternative picture of hybrid mesons, one supported by lattice QCD [2], is one in which a gluonic flux tube forms between the quark and antiquark and the excitations of this flux tube lead to so-called hybrid mesons. Conventional  $q\bar{q}$  mesons arise when the flux tube is in its ground state. Hybrid mesons arise when the flux tube is excited and some hybrid mesons can have a unique signature, exotic  $J^{PC}$ , and the spectroscopy of these exotic hybrid mesons is simplified because they do not mix with conventional  $q\bar{q}$  states. Lattice calculations presented later (section III) support the existence of exotic-quantum-number states within the meson spectrum, independent of specific models.

The GlueX experiment (shown in Figure 1) has been designed to make these measurements on the existence of these hybrid states. A program in spectroscopy, supported by a sophisticated amplitude analysis, will map out the spectrum of the exotic-quantum-number states on top of the background of normal  $q\bar{q}$  mesons. Detailed comparisons to theoretical predictions will provide experimental information on the excitations of the gluonic field in mesonic systems, and lead to a more detailed understanding of the role of glue in the confinement of quarks inside hadronic matter.

---

\* Spokesperson: Curtis A. Meyer, (cmeyer@cmu.edu)

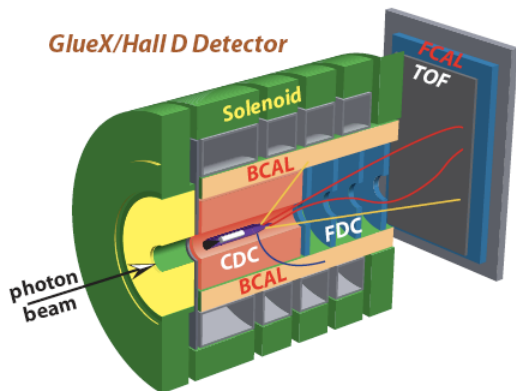


FIG. 1. The GlueX detector.

## II. MESON SPECTROSCOPY AND THE SEARCH FOR QCD EXOTICS

The experimental search for exotic hybrids continues, but the data supporting the existence of these states are still sparse. Recent review articles [3–5] provide a good summary of the status of the field, but the bottom line is that evidence exists for up to three isospin-one,  $J^{PC} = 1^{-+}$ , exotic-quantum-number states:  $\pi_1(1400)$ ,  $\pi_1(1600)$  and  $\pi_1(2015)$  (whose properties are summarized in Table I). Of these states, the  $\pi_1(1400)$  is almost certainly not a hybrid meson, and may not be a resonance. The  $\pi_1(1600)$  and the  $\pi_1(2015)$  are both potential candidates for hybrid mesons. The  $\pi_1(1600)$  suffers from a number of inconsistencies in its production, which appears different depending on how it decays. There is also a good deal of controversy about its  $\rho\pi$  decay, with the existence of the decay mode apparently strongly dependent on assumptions in the analysis. However, overall there is fairly strong evidence this state exists. The highest-mass state is the result of very-low statistics data sets from E852 and needs confirmation. If both of these higher-mass states exist, they could be explained as the ground and first-excited states of this system, a result which may be consistent with recent lattice calculations discussed below.

As noted above, the  $\rho\pi$  ( $3\pi$ ) decay mode of the  $\pi_1(1600)$  remains controversial. In 2005, a high-statistics analysis of E852 data showed that the signal for the  $\pi_1(1600)$  went away when known decays of the clearly-seen  $\pi_2(1670)$  were included in the partial wave analysis. A CLAS analysis of photo-production data to the  $3\pi$  final state also failed to see the  $\pi_1(1600)$  in its  $3\pi$  decay mode [8]. Finally, the VES experiment was never able to confirm the  $3\pi$  decay of the  $\pi_1(1600)$ . While the  $\pi_1(1600)$  appears solid via its other decay modes, the simple  $3\pi$  mode has been called into question. Re-

State	Mass (GeV)	Width (GeV)
$\pi_1(1400)$	$1.351 \pm 0.03$	$0.313 \pm 0.040$
$\pi_1(1600)$	$1.662 \pm 0.015$	$0.234 \pm 0.050$
$\pi_1(2015)$	$2.01 \pm 0.03$	$0.28 \pm 0.05$
State	Production	Decays
$\pi_1(1400)$	$\pi^- p, \bar{p}n$	$\pi^- \eta^\ddagger, \pi^0 \eta^\ddagger$
$\pi_1(1600)$	$\pi^- p, \bar{p}p$	$\eta' \pi, b_1 \pi, f_1 \pi, \rho \pi^\ddagger$
$\pi_1(2015)$	$\pi^- p$	$b_1 \pi, f_1 \pi$
State	Experiments	
$\pi_1(1400)$	E852, CBAR	
$\pi_1(1600)$	E852, VES, COMPASS, CBAR	
$\pi_1(2015)$	E852	

TABLE I. The three exotic-quantum-number states for which some experimental evidence exists. The masses and widths are the Particle Data Group average [6]. The decays with a superscript  $\ddagger$  are considered controversial.

cently, the COMPASS experiment at CERN published their first results  $3\pi$  final states produced in peripheral pion production on nuclear targets [9, 10]. Even including the extra decays of the  $\pi_2(1670)$ , they report signal for the  $\pi_1(1600)$  in  $3\pi$ , which is shown in Figure 2. However, the COMPASS results are somewhat surprising in that both the  $\pi_2(1670)$  and the  $\pi_1(1600)$  have virtually the same mass and width. This is most clearly seen by the nearly flat phase motion between these states shown in Figure 2 and leads to concerns that the exotic state may be the result of unaccounted for feed-through from the stronger  $\pi_2$  state, possibly caused by the use of the isobar model.

While there is evidence for the isospin-one member of the  $J^{PC} = 1^{-+}$  nonet, we also expect two isospin-zero states, ( $\eta_1$  and  $\eta_1'$ ) as well as two additional exotic nonets with  $J^{PC} = 0^{+-}$  and  $2^{+-}$ . There is still no experimental evidence for any of these other states. The former are necessary to establish the nonet nature of the  $\pi_1$  states, and the latter are expected in most models of hybrids. Table II lists the nine expected exotic-quantum number states as well as model predictions for their widths and decay modes. Finding many of the mapping of these missing states remains a crucial activity.

Over the next several years, we anticipate that COMPASS will have new results based on their large data set which was collected on a proton target. These could indeed be very interesting, but they will be extensions of the diffractive pion production data collected by E852 and VES, albeit at higher beam energies. In addition to the diffractive production, COMPASS will also study central production, a program aimed at extending the work of the CERN WA102 experiment on the search for glueballs. We hope that COMPASS will be able to resolve the inconsistencies surrounding the  $\pi_1(1600)$  in an unambiguous fashion. There is also hope that confirmation might be seen for the  $\pi_1(2015)$  and other states

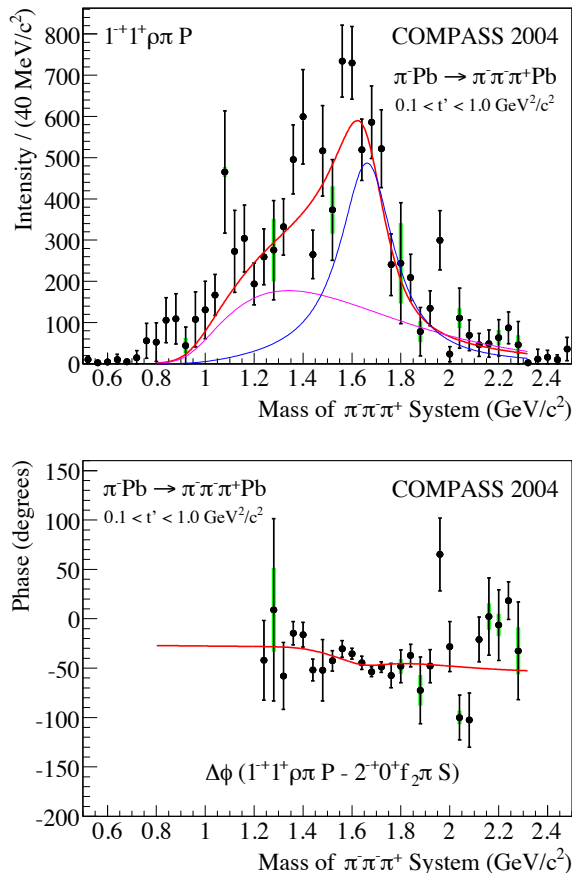


FIG. 2. The upper plot shows the intensity of the spin-exotic  $1^{-+} \rho \pi$  partial wave. The red curve shows the result of a mass-dependent fit with one Breit-Wigner for the  $\pi_1(1600)$  (blue curve) on top of an unexplained background (purple curve). The lower curve shows the phase difference between the  $1^{-+}$  ( $\pi_1(1600)$ ) and the  $2^{-+}$  ( $\pi_2(1670)$ ) partial waves. Figure is taken from reference [10].

may be found, however, the production mechanism is still limited to that studied in earlier experiments (E852 and VES), and may not provide a complete picture.

In addition to COMPASS, BES-III in Beijing has now been running for nearly a year, and their data sets of  $\psi$  states now exceed the world data sets in a number of areas by large factors. While they are not able to directly produce hybrid  $\bar{c}c$  states, they may be able to accumulate enough statistics to start teasing out signals with a full PWA of the decays of higher mass  $\chi_c$  states. They may also be able to search for light-quark hybrids from the decays of the lighter  $\chi_c$  states. Although, the branching fractions probably lead to a reduction of about  $10^6$  of the initial  $\psi$  state to the light-quark-hybrid. This will indeed be challenging and the ultimate answer on  $c\bar{c}$  hy-

Name	$J^{PC}$	Total Width MeV		Large Decays
		PSS	IKP	
$\pi_1$	$1^{-+}$	81 – 168	117	$b_1\pi, \rho\pi, f_1\pi, a_1\eta$
$\eta_1$	$1^{-+}$	59 – 158	107	$a_1\pi, f_1\eta, \pi(1300)\pi$
$\eta'_1$	$1^{-+}$	95 – 216	172	$K_1^m K, K_1^l K, K^* K$
$b_0$	$0^{+-}$	247 – 429	665	$\pi(1300)\pi, h_1\pi$
$h_0$	$0^{+-}$	59 – 262	94	$b_1\pi, h_1\eta, K(1460)K$
$h'_0$	$0^{+-}$	259 – 490	426	$K(1460)K, K_1^l K, h_1\eta$
$b_2$	$2^{+-}$	5 – 11	248	$a_2\pi, a_1\pi, h_1\pi$
$h_2$	$2^{+-}$	4 – 12	166	$b_1\pi, \rho\pi$
$h'_2$	$2^{+-}$	5 – 18	79	$K_1^m K, K_1^l K, K_2^* K$

TABLE II. Exotic quantum number hybrid width and decay predictions from reference [11]. The column labeled PSS (Page, Swanson and Szczepaniak) is from their model, while the IKP (Isgur, Karl and Paton) is their calculation of the model in reference [12]. The variations in width for PSS come from different choices for the masses of the hybrids. The  $K_1^l$  represents the  $K_1(1270)$  while the  $K_1^m$  represents the  $K_1(1400)$ .

brids may well have to wait for the PANDA program (at GSI) which will probably start production running somewhat after GlueX.

### III. MESON SPECTROSCOPY AND LATTICE QCD

During the last five years, there have been several theoretical advances in our understanding of hybrid mesons. Most significant has been recent lattice QCD (LQCD) work which predicts the entire spectrum of light-quark mesons [13, 14]. The fully dynamical (unquenched) calculation is carried out with two flavors of light quarks and a heavier one tuned to the strange quark mass on two lattice volumes and four masses for the light quarks. These correspond to pion masses of 700, 520, 440 and 390 MeV, where the heaviest case has the three quark masses the same at the strange mass. For the heaviest case, the computed spectrum of isovector states are shown in Figure 3 (where the mass is plotted as a ratio to the  $\Omega$ -baryon mass (1.672 GeV)). In the plot, the right-most columns correspond to the exotic  $\pi_1, b_0$  and  $b_2$  states. Interesting to note is that the  $1^{-+} \pi_1$  is the lightest, and that both a ground state and what appears to be an excited state are predicted. The other two exotic-quantum number states appear to be somewhat heavier than the  $\pi_1$  with an excited state for the  $b_2$  visible.

Beyond the scale of this calculation, there are a number of important innovations. First, the authors have found that the reduced rotational symmetry of a cubic lattice can be overcome on sufficiently fine lattices. They used meson operators of definite continuum spin subduced into the irreducible representations of cubic

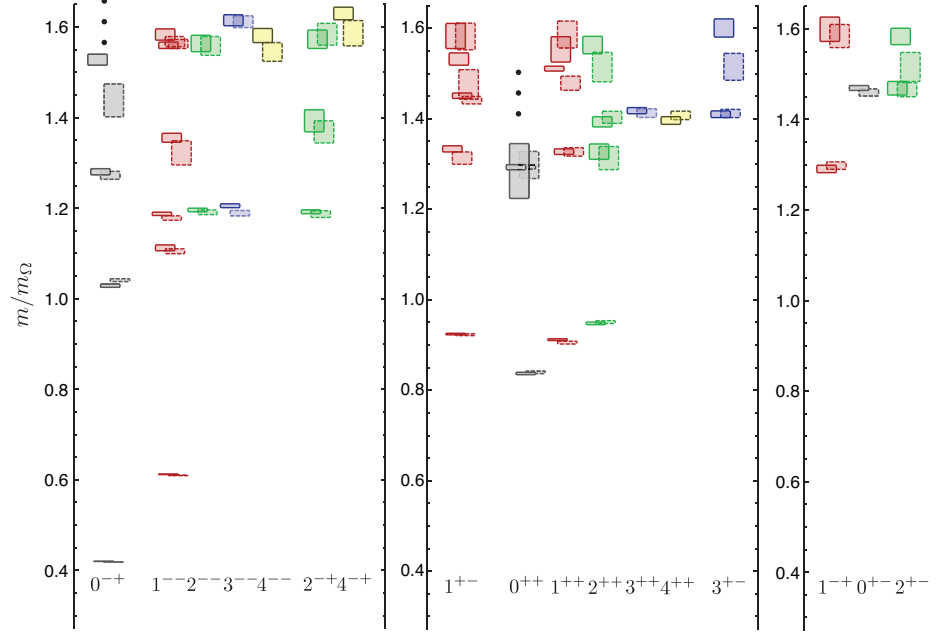


FIG. 3. The LQCD prediction for the spectrum of isovector mesons. The quantum numbers are listed across the bottom, while the color denotes the spin. Solid (dashed) bordered boxes on a  $2.0^3(2.4^3)$  fm volume lattice, little volume dependence is observed. The three columns at the far right are exotic-quantum numbers. The plot is taken from reference [14].

rotations and observed very strong correlation between operators and the spin of the state. In this way they were able to make spin assignments from a single lattice spacing. Second, the unprecedented size of the operator basis used in a variational calculation allowed the extraction of a great many excited states with confidence.

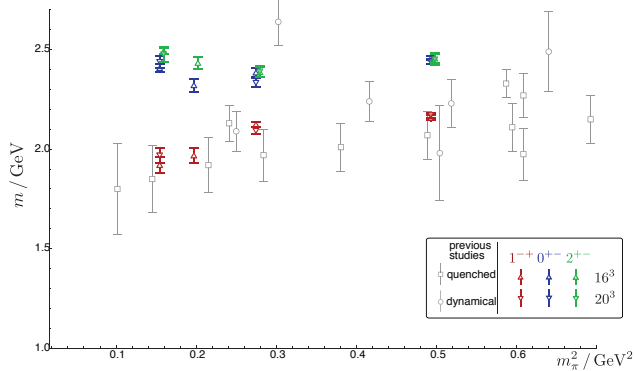


FIG. 4. The mass of the isovector exotic states as a function of  $m_\pi^2$  used as a proxy for the light quark mass. Data are taken from reference [14].

There were also phenomenological consequences of these lattice results. A subset of the meson operators used features the commutator of two gauge-covariant

derivatives, equal to the field-strength tensor which is non-zero only for non-trivial gluonic field configurations. Large overlap onto such operators was used to determine the degree to which gluonic excitations are important in the state, *i.e.* what we would call the *hybrid* nature of the state. In particular, the exotic quantum number states all have large overlap with this type of operator, likely indication hybrid nature over, say, multiquark structure.

In order to be able to extract the masses of states to be comparable with experiment, it is necessary to work at the physical pion mass. While work is currently underway to extract a point at  $m_\pi \sim 280$  MeV, it will still be a little while before this limit is reached. To attempt to extrapolate, one can plot the extracted state masses as a function of the pion mass squared, which acts as a proxy for the light quark mass (see Figure 4). While linearly extrapolating to the physical pion mass ignores too much expected physics, it is probably safe to say that both the  $\pi_1(1600)$  and the  $\pi_1(2015)$  could be consistent with the expected  $1^{-+}$  mass, and that the  $b_0$  and  $b_2$  masses will likely be 200 to 300 MeV heavier. These masses are all within the designed mass reach of GlueX.

Perhaps the most striking element of this calculation is the strong correlation with quark model predictions for the normal  $q\bar{q}$  states [15], but only if they are supplemented with *non-exotic* hybrid meson states. The flux-tube model is an example of a framework which includes both the conventional and hybrid states in a seamless

way. In the non-exotic  $J^{PC} = 1^{--}$  sector, the lattice calculations extract six states (shown in Figure 3 near 0.7, 1.1, 1.2, 1.3, 1.55 and  $1.6 m_\Omega$ ). The quark model predicts five conventional states in this mass region,  $1^3S_1$ ,  $1^3S_1$ ,  $1^3D_1$ ,  $3^3S_1$  and  $2^3D_1$ . In examining the operator content of the lattice states, the state near 1.3 has a large overlap with operators requiring a non-trivial gluonic field component, while the other states mostly do not. We also note that the state at 1.3 roughly lines up in mass with the exotic quantum numbered states. This is compatible with the picture suggested by the flux-tube model amongst others.

Similarly, in the  $J^{PC} = 2^{-+}$  sector ( $\pi_2$ ), the quark model predicts two states, the  $1^1D_2$  and the  $2^1D_2$  while the excited flux-tube model adds a non-exotic hybrid state. The lattice calculations indeed show three states, at 1.2, 1.4 and  $1.6 m_\Omega$ , with the middle one having a large overlap with the non-trivial gluonic-field operators. There also appears to be a hybrid pseudoscalar and possibly positive parity non-exotic hybrid states.

These recent lattice calculations are extremely promising. They reaffirm that hybrid mesons form part of the low-energy QCD spectrum and that exotic quantum number states exist. They also provide, for the first time, the possibility of assessing the gluonic content of a calculated lattice state. Similar calculations are currently underway for the isoscalar sector where preliminary results [16] for the mass scale appear consistent with those shown here in the isovector sector. These calculations will also extract the flavor mixing angle, an important quantity for phenomenology.

There are also new theoretical calculations relevant to the photo production of hybrid mesons. Lattice calculations in the charmonium sector looked at radiative decays of  $c\bar{c}$  states [17, 18]. Rates were computed for a number of decays of conventional  $c\bar{c}$  states, and found to be in quite reasonable agreement with experiment, thus yielding confidence in the calculation and the procedure of extracting rates. Based on this, the radiative decay of the  $1^{-+}$  hybrid charmonium state ( $\eta_{c1}$ ) to  $J/\psi\gamma$  was computed. The rate was found to be large on the scale of conventional decays, and to proceed dominantly through an magnetic-dipole ( $M1$ ) transition. This transition involves a spin-flip for normal  $c\bar{c}$  states and is typically suppressed by the heavy charm-quark mass. In the hybrid system, no spin-flip appears to be needed as the gluonic field provides the one unit of angular momentum within a quark spin-triplet hybrid. Work is underway to extend these calculations to the light-quark sector where they will be directly applicable to GlueX. However, the charmonium results tend to confirm the suggestions of the flux-tube model [19, 20], that hybrid meson photo-production is at least as large as that of normal  $q\bar{q}$  states.

#### IV. GLUEX DATA ANALYSIS

A full GEANT model of Hall-D/GlueX (HDGEANT) starting from the bremsstrahlung target and continuing through the GlueX detector exists and has been used extensively to model background rates in the detector as well as study physics reactions in GlueX. The Monte Carlo can be fed with a number of event generators, including a tuned version of the PYTHIA [27] that can simulate the entire photo-hadron cross section and is used to produce background event samples. The events from HDGEANT can be fully reconstructed and used to study physics processes, optimize detector design, and understand the impact of changes to the detector system. The running of our simulation has taken advantage of work done by our collaboration implement Open Science Grid (OSG) software for GlueX. Currently we are able to run Monte Carlo simulation for GlueX on the grid and our data is cached and retrieved from grid storage.

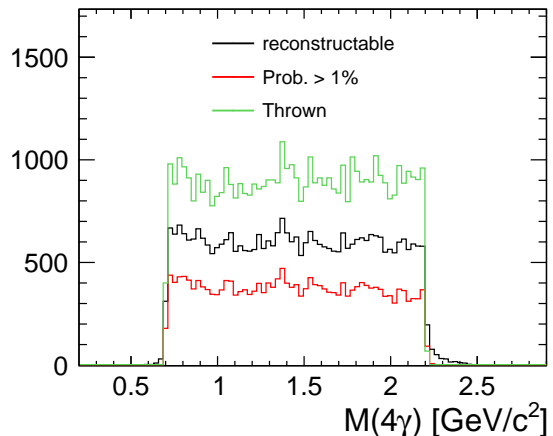


FIG. 5. The  $\gamma\gamma\gamma\gamma$  invariant mass from reference [28]. The green curve represents the generated events, the black curve are those that are reconstructable (about 65 to 70%), while the red curve are those events which satisfy a six-constraint kinematic fit at the 1% confidence level (about 45%).

Using these tools, a full analysis of the reaction  $\gamma p \rightarrow p\eta\pi^0$  (as part of the first Ph.D. thesis on GlueX [28]) has been carried out. This analysis mixed a Monte Carlo  $\eta\pi$  event sample with a full sample of PYTHIA background events. The events were then passed through the HDGEANT simulation and reconstructed using the GlueX/Hall-D analysis code. The resulting events were then further processed using kinematic fitting combined with various kinematic cuts to separate signal from background. Thus, the analysis represents the most complete and accurate analysis of GlueX data to date. While not fully optimized, the acceptance for a final state with four photons and a proton is around 50% after kinematic fit-

ting and all current analysis cuts. This is shown in Figure 5 where the curves represent the thrown sample, the reconstructable sample, and the sample after kinematic fitting to the  $\eta\pi^0 p$  final state. This analysis also obtains a signal to background ratio for the  $\eta\pi^0$  events on top of the PYTHIA background that is typically between two and five. The major limitation at the moment is due to clustering in the calorimeters and photons being *split* over more than one clusters. Based on this analysis, work is focusing on improving these algorithms as well.

As a historical note, at the time of our original PAC presentation, virtually no reconstruction software existed, and all studies were carried out using a (now retired) fast Monte Carlo package from FNAL. The current situation is a full simulation, reconstruction and much of a physics analysis package. The questions now being addressed in the software are on issues of global analysis and speed. Recently, the issue of *hadronic split-offs* in the calorimeter has come to the forefront. Here, a charged particle interacting in the calorimeter may produce secondaries (neutrons) that travel far from the initial impact point before depositing more energy. We believe that the excellent timing in all of our calorimeters will play a significant role in solving this problem. We are also exploring more sophisticated tracking algorithms (Kalman filters) to attempt to improve our overall resolution. Finally, as discussed above, our analysis software is to the point where full physics analyses can now be undertaken. Finally we note that a standard event sample ( $b_1\pi$ ) events is now automatically run through the analysis chain on regular basis to monitor the stability of the code.

## V. GLUEX AMPLITUDE ANALYSIS

The discovery of exotic-quantum-number mesons in the photo-production data from GlueX hinges on an amplitude analysis to extract the signals. These analyses will take as input measured four-vectors of both reconstructed and simulated events. A unbinned maximum likelihood fit is then used to determine the physics model which makes the real and simulated event distributions agree. The physics model includes both known processes, possible new mesons and backgrounds, with the crucial extracted signal being intensities and phase differences. If these are robust over several related final states, it is then possible to extract masses and widths of mesons from the data.

An example of this comes from a recent analysis on the photo production of  $\omega$  mesons in CLAS [26]. This was carried out by GlueX collaborators who are also members of CLAS using analysis tools that were developed to be useful for GlueX. Figure 6 shows the strength of the dominant waves in the data (upper) and the phase difference between two  $s$ -channel contributions (lower). The phase difference requires two nearby  $J^P = (\frac{5}{2})^+$  resonances to describe it. The lower is the four-star

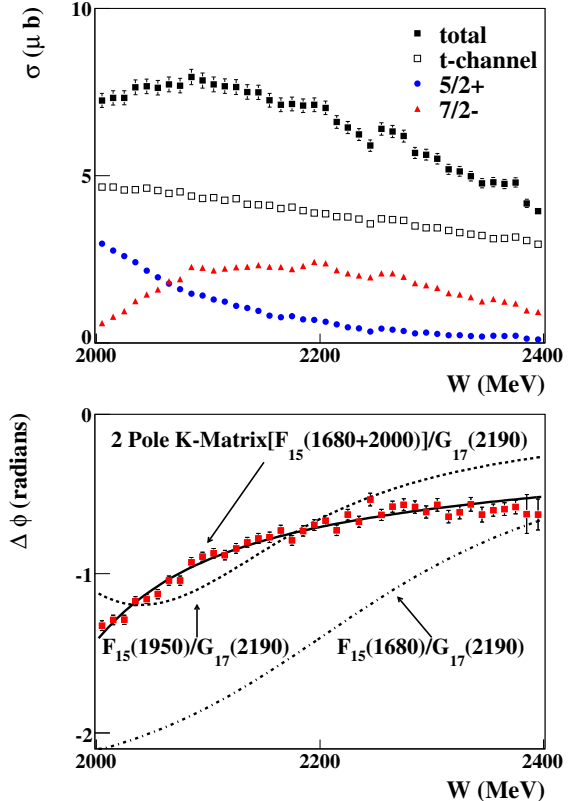


FIG. 6. Results from the partial wave analysis of  $\gamma p \rightarrow \omega p$ . The upper plot shows the intensity of the contributions to the total cross section, with the dominant signals being  $t$ -channel pion exchange, and  $J^P = (\frac{5}{2})^+$  and  $(\frac{7}{2})^-$  partial waves. The lower figure shows the phase difference between the two  $s$ -channel waves, which requires two interfering  $(\frac{5}{2})^+$  resonances to describe the data. The plots are taken from reference [26].

$F_{15}(1680)$  while the higher-mass state is an  $F_{15}(1950)$ , a state that is considered one of the *missing baryons*. The interference with the  $(\frac{7}{2})^- G_{17}(2190)$  is crucial in extracting this result.

The amplitude analysis tools which were developed for photo production in CLAS are available to carry out PWA in GlueX. As part of an NSF Physics at the Information Frontier (PIF) grant, work has been done to improve parallelization and look at porting the code to the OSG. Also, as part of the PIF, work has been done to improve the theoretical underpinnings of the amplitudes used in the amplitude analysis. While this improves the physics, it also increases the computational complexity of these, and thus impacts the analysis time. Because of this, we have also carried out work to implement and test amplitude analysis on graphical processor units (GPUs). GPUs are very effective at handling highly parallel, computationally intense calculation that involve

minimal data movement—all of which describes an amplitude analysis. Early results look extremely promising and we are proceeding in this direction.

Currently, we are pursuing several different amplitude analyses simultaneously. These are focused on channels which we have identified as the *best* first physics analyses. The  $3\pi$  system is being looked at in the framework of our improved amplitudes, with the code running on GPUs and is being carried out by collaboration members with experience in both CLEO and E852 analyses. We are also looking at the  $b_1\pi$  system using the tools developed for CLAS analyses. This is being carried out by collaboration members with experience in both CLAS and Crystal Barrel amplitude analyses. We also have other groups looking at various aspects of these analyses. All of these follow a plan where a physics signal in an interesting final state is mixed with the appropriate amount of hadronic background (PYTHIA) events. The data are then simulated, reconstructed, and our best tools are used to isolate the desired signal. This signal is then sent to an amplitude analysis and the results will be compared to the input physics model. While this is currently underway, we believe that we are still several months away from our first full results.

## VI. UPDATES TO THE GLUEX EQUIPMENT

During the last 4 years, the GlueX experiment and Hall-D have gone through extensive reviews as part of the Department of Energy’s *Critical Decision* process. These external reviews focused on all aspects of the detector and the results not only vetted the design of the detector, but also led to a number of design changes which improved GlueX and reduced risk and cost. Because of the closely coupled nature of both GlueX and Hall-D, the collaboration has been a very active participant in all of these reviews, a (probably incomplete) list of which can be found in Table III. As a result of the review process, there have been a number of changes to the GlueX detector as discussed below.

Figure 1 shows a cut-away view of the GlueX detector. Not shown is the tagger hall where the 9 GeV linearly-polarized photon beam is produced via the coherent bremsstrahlung process in a thin ( $20\ \mu\text{m}$ ) diamond crystal. The scattered electron from the bremsstrahlung process is detected in a tagger system instrumented with a very fine scintillator system (the microscope) at the coherent peak, and a coarser grained system spanning most of the remaining energy range. After travelling 80 meters, the photon beam is scraped using a 3 mm diameter active collimator (to assist beam tuning), and then passes through a pair spectrometer system for monitoring flux, energy and polarization.

The photons then interact in a liquid-hydrogen target and the resulting charged particles and photons are detected in GlueX. Charged particles travel through a

Review	Date
Drift chamber review	March 2007
FDC technology review	February 2008
Calorimeter design review	February 2008
Tracking and PID final design review	March 2008
System and infrastructure design review	May 2008
IPR Lehmann review	July 2008
Beamline and tagger review	November 2008
Installation review	February 2009
Tagger magnet design review	July 2009
BCAL readout review	July 2009
Solenoid magnet internal review	Nov 2009
Solenoid review	April 2010

TABLE III. A list of the GlueX/Hall-D externals reviews which were part of the DOE decision process.

scintillating fiber start counter which is just outside the target volume. They are then tracked through the 2.2 T solenoidal field in the central drift chamber (CDC) and the forward drift chamber (FDC) packages. Time-of-flight is measured in the forward TOF system as well as in the BCAL. Inside the magnet bore, photons are detected in a lead-scintillating fiber calorimeter (BCAL) where the signals are read out using field-insensitive silicon photomultipliers (SciPMs). In the forward direction, photons are detected in a lead-glass calorimeter (FCAL) which is down-stream of the TOF.

The most significant change to the GlueX detector has been the *descope* of the Cerenkov system for particle identification. This was done by the project to increase contingency funds for the rest of the project. The collaboration is actively seeking new groups who would take on this system on funds outside of the 12-GeV project. Either as an NSF MRI project, or possibly as part of post-CD4 detector improvements.

Improvements and changes have also been made to many of the detector systems in Hall-D and GlueX. In the tagger system, the original two-magnet design has been replaced by a single magnet which reduces cost and improves alignment issues. Solenoid: A major overhaul has been performed on the GlueX solenoid. This has been necessary to fix a number of leaks and shorts in the system. The iron yolk has been redesigned to fill gaps in the earlier design. This improves the overall magnetic field shape, and reduces the amount of saturated magnetic material. In order to improve the overall tracking efficiency and the resolution of the detector, the CDC has been shortened by about 10%, the fraction of stereo layers has been increased and a tighter packing of the straws has led to an increase in the number of layers by four. To reduce material in the tracking volume, the down stream endplate is thinner and made of carbon fiber. The FDC has had significant material removed from the tracking volume. A full-scale prototype

Contract	Group	Status
Tagger	UCONN	in process
Tagger	Catholic	in process
Tagger	NCA& T	in process
Pair Spect.	UNC Wilmington	in process
Target	UMASS	in process
Start Counter	FIU	in process
CDC	CMU	in place
FDC	JLab	in place
FDC	UVA	in process
BCAL	U. Regina	in place
BCAL Readout	Santa Maria	in process
TOF	FSU	in process
FCAL	I.U.	in place
Solenoid	JLab	in place
Solenoid	IUCO	in place
Trigger	CNU	in process
Electronics	JLab	in place
Electronics	UMASS	in process

TABLE IV. The construction contracts for GlueX.

of a module was just completed at Jefferson Lab. A final decision was made to readout the BCAL using silicon photomultipliers (SiPMs). These form a compact readout that is very close to the detector which eliminates light guides and is insensitive to the magnetic field. We have also found that the attenuation length of the scintillating fibers is exceeding specification by a large margin. Both of these effects lead to improved light collection and thus, detector performance. For the TOF, we will be using a faster photomultiplier tubes to improve timing and a somewhat thicker scintillator to better match the photomultiplier size. In the FCAL, the use of silicon cookies to optically connect the lead-glass crystals to the photomultipliers has improved light collection and thereby the detector performance. It has also been decided to adopt the PrimEx scheme of stacking the crystals, simplifying the support frame and reducing costs.

Construction has started on the BCAL, the FCAL and the CDC, and the first four (of 48) BCAL modules have been delivered to Jefferson Lab. Construction on other elements will start over the next two years at institutions around the world. A summary of the construction contracts needed to build GlueX is shown in Table IV. Finally, based on the detailed prototype work carried out for GlueX, we have continued to publish instrumentation papers. From work on the BCAL, results of our beam test in Hall-B [21] as well as information on the spectral response of scintillating fibers [22] have been published. We also have written an article on the CDC [23] and one is approaching submission on the the FCAL [24].

## VII. OTHER PHYSICS USING GLUEX/HALL-D

It has long been recognized by us that much physics beyond meson spectroscopy and the search for exotics will be possible in Hall-D and GlueX. In March of 2008, the collaboration organized a workshop [29] at Jefferson Lab, “Photon-hadron physics with the GlueX detector at JLab” that was attended by about 70 people. A number of interesting ideas came out of this meeting and one has matured to an accepted proposal. The PrimEx experiment at 12-GeV was approved by PAC-35 to run using the Hall-D beamline and the GlueX detector. The proponents of this proposal have joined GlueX and the collaboration as a whole worked on the final proposal that was submitted in December 2009.

Other physics topics that are maturing within the collaboration include baryon spectroscopy. In particular, the spectrum of double-strange Cascade baryons. These are poorly known with only a few resonances that are well established. Many more states must exist; if not, our understanding of baryon structure is fundamentally flawed. It would be interesting to see the lightest excited  $\Xi^*$  states in certain partial waves decoupling from the  $\Xi\pi$  channel confirming the flavor independence of confinement. Measurements of the isospin splittings in spatially excited Cascade states are also needed. Currently, these splittings like  $n - p$  or  $\Delta 0 - \Delta^{++}$  are only available for the octet and decuplet ground states, but are hard to measure in excited  $N$ ,  $\Delta$  and  $\Sigma$ ,  $\Sigma^*$  states, which are very broad. Many cascade baryons are likely to be narrow and measuring the  $\Xi^- - \Xi 0$  splitting of spatially excited  $\Xi$  states remains a strong possibility. These measurements are an interesting probe of excited hadron structure and would provide important input for quark models which are describing the isospin splittings by the  $u$ - and  $d$ -quark mass difference as well as by the electromagnetic interactions between the quarks.

Other interesting ideas such as inverse DVCS and threshold charm production still require additional work to flesh out a physics program.

## VIII. SUMMARY

The experimental search for exotic-quantum-number mesons continues to be an exciting problem, albeit one which continues to be limited by the lack of data. Data support the picture of two isospin-one  $J^{PC} = 1^{-+}$  states, the  $\pi_1(1600)$  and the  $\pi_1(2150)$ . However, limited statistics mean that confirmation is needed, particularly for the higher-mass state. Recent progress in LQCD reaffirms the existence of exotic-quantum-number mesons, and their large overlap to *non-trivial* gluonic fields. It also predicts the existence of normal quantum number hybrids and provides a method of measuring the overlap with the gluonic fields, all of this independent of specific models of QCD. Other LQCD calculations support the



picture that photo production is indeed a good place to search for hybrid mesons. These calculations also suggest that two isospin-one  $J^{PC} = 1^{-+}$  states are expected, but many unobserved states are also expected.

Over the next several years, we anticipate additional results from the COMPASS experiment at CERN which will continue to explore the diffractive pion production studied by E852 and VES. We also may have some results from the BES-III experiment on both charmonium- and

light-quark-hybrids, but statistics may be limited. At about the same time that GlueX begins to produce results, the PANDA experiment at GSI is expected to start searching for both glueballs and charmonium hybrids in proton-antiproton annihilations. GlueX remains and will remain *the* high-statistics experiment for light-quark hybrids which will explore a new production mechanism and are on track to be able to start doing *physics* in 2015 when the first production-like beams become available.

- 
- [1] The GlueX Collaboration, “Mapping the Spectrum of Light Quark Mesons and Gluonic Excitations with Linearly Polarized Photons”, GlueX-doc 1226, January (2006), (<http://argus.phys.uregina.ca/cgi-bin/public/DocDB/ShowDocument?docid=1226>).
- [2] G. S. Bali *et al.* [TXL Collaboration and T(X)L Collaboration], Phys. Rev. D **62**, 054503 (2000).
- [3] Eberhard Klempt and Alexander Zaitsev, Phys. Rep. **454**, 1, (2007).
- [4] V. Crede and C. A. Meyer, Prog. Part. Nucl. Phys. **63**, 74 (2009).
- [5] C. A. Meyer and Y. Van Haarlem, submitted to Phys. Rev. C, (2010), arXiv:1004.5516 [nucl-ex].
- [6] C. Amsler, *et al.* [The Particle Data Group], Phys. Lett. B **667**, 1, (2008).
- [7] A. R. Dzierba *et al.*, Phys. Rev. D **73**, 072001 (2006).
- [8] M.Nozar *et al.* [CLAS Collaboration], Phys. Rev. Lett. **102**, 102002, (2009).
- [9] A. Alekseev *et al.* [The COMPASS Collaboration], arXiv:0910.5842 [hep-ex] (2009).
- [10] B. Grube *et al.* [The COMPASS Collaboration], arXiv:1002.1272 [hep-ex] (2010).
- [11] P. R. Page, E. S. Swanson and A. P. Szczepaniak, Phys. Rev. D **59**, 034016 (1999).
- [12] N. Isgur, R. Kokoski and J. Paton, Phys Rev. Lett. **54**, 869, (1985).
- [13] J. J. Dudek, R. G. Edwards, M. J. Peardon, D. G. Richards and C. E. Thomas, Phys. Rev. Lett. **103**, 262001 (2009).
- [14] J. J. Dudek, R. G. Edwards, M. J. Peardon, D. G. Richards and C. E. Thomas, submitted to Phys. Rev. D, (2010), arXiv:1004.4930 [hep-ph].
- [15] S. Godfrey and N. Isgur, Phys. Rev. D **32**, 189 (1985).
- [16] J. J. Dudek, private communication.
- [17] J. J. Dudek, R. G. Edwards and D. G. Richards, Phys. Rev. D **73**, 074507 (2006).
- [18] J. J. Dudek, R. Edwards and C. E. Thomas, Phys. Rev. D **79**, 094504 (2009).
- [19] F. E. Close and J. J. Dudek, Phys. Rev. Lett. **91** (2003) 142001
- [20] F. E. Close and J. J. Dudek, Phys. Rev. D **69** (2004) 034010
- [21] B.D. Leverington *et al.*, Nucl. Instrum. Methods A **596**, 327 (2008).
- [22] Z. Papandreou, B.D. Leverington and G.J. Lolos, Nucl. Instrum. Methods A **596**, 338 (2008).
- [23] Y. Van Haarlem, C.A. Meyer, *et al.*, Accepted for publication in Nucl. Instrum. Methods, arXiv:1004.3796 [nucl-ex], (2010).
- [24] J. Bennett, M. Kornicer, M. Shepherd *et al.*, to be submitted to Nucl. Instrum. Methods (2010).
- [25] M. Williams, Comp. Phys. Comm. **180**, 1847, (2009).
- [26] M. Williams *et al.* [CLAS Collaboration], Phys. Rev. C **80**, 065209 (2009).
- [27] <http://home.thep.lu.se/~torbjorn/Pythia.html>.
- [28] Blake D. Leverington, “The GlueX lead-scintillating fibre electromagnetic calorimeter”, Ph.D. Thesis, University of Regina, (2010).
- [29] <http://www.jlab.org/Hall-D/meetings/php2008/program.html>.